Velocity Profiles of Current and Low GWP Propellant pMDI Spray Plumes

Benjamin Myatt[1] **& Hossain Chizari**[1]

[1] Kindeva Drug Delivery, Charnwood Campus, Loughborough, UK

Summary

The pharmaceutical industry is switching to low global warming potential (GWP) propellants HFA152a or HFO1234ze(E) to reduce the carbon footprint of pressurised metered dose inhalers (pMDIs). The physicochemical properties of these propellants play a critical role in governing the atomisation and plume evolution processes and consequently product performance. The velocity of a spray plume as it exits a pMDI plays a critical role in governing atomised droplet size and is highly dependent on propellant properties. Further downstream, differences in velocity of the spray plume and inhaled co-flow can lead to mixing induced turbulent diffusion and differences in oropharyngeal deposition.

Measurements of pMDI plume velocities of HFA134a, HFA227ea, HFA152a and HFO1234ze(E) propellants emitted from a Kindeva pMDI actuator showed broadly similar velocity profiles both in trend and magnitude through the plume centreline, a vertical plane 25 mm from the actuator mouthpiece and temporally in the centre of the plume at the same distance.

Key Message

Radial and axial distributions of pMDI spray plume velocities of current high GWP propellants HFA134a and HFA227ea and low GWP propellants HFA152a or HFO1234ze(E) were found to be broadly similar with only minor differences observed between propellants.

Introduction

Evolving legislation and a desire to reduce carbon footprint of pMDIs (pressurised metered dose inhalers) is driving the switch from current high GWP (global warming potential) propellants HFA134a and HFA227ea to low GWP propellants HFA152a or HFO1234ze(E) [1]. The physicochemical properties of these propellants differ with some key parameters summarised in Table 1. These parameters play critical roles in governing atomisation of respirable droplets, the aerosol velocity and evolution processes and consequently pMDI product performance [2].

pMDI atomisation is predominantly due to an aerodynamic mechanism, with significant flashing of the volatile propellant [3]. Velocity of the two-phase formulation mixture as it exits the spray orifice is a key parameter in governing resultant droplet size: higher exit velocities lead to smaller droplet sizes. Further downstream, the velocity of the spray plume inhaled by a patient impacts the amount of oropharyngeal deposition. A mismatch of plume velocity compared to that of inhaled airflow induces turbulent mixing in a patient's oral cavity and high plume velocities cause high oropharyngeal deposition [4,5].

Understanding the impact of switching to low GWP propellants on pMDI plume velocity may unlock further understanding of pMDI product performance and aid a successful transition of products to these new propellants. Previous studies have characterised velocity profiles of high GWP propellant pMDI sprays both temporally and spatially [6,7,8,9]. In-depth analyses of these data have been reported discussing the impact of propellant properties on the pMDI atomisation mechanism and resultant pharmaceutical product performance. However, there is little experimental data in the literature detailing the velocity of low GWP propellant pMDI sprays, limited to a small number of datapoints measured along the plume axis [10]. In this study the velocity of pMDI sprays of HFA134a, HFA227ea, HFA152a and HFO1234ze(E) propellants were measured and their velocity profiles compared. The particle image velocimetry (PIV) technique was used owing to its ability, unlike with plume front velocity measurements, to capture information about the temporal nature and spatial and evolution of the pMDI spray plume.

Table 1: Properties of current high GWP and low GWP pMDI propellants

Property	**HFA134a** [11]	**HFA227ea** [12]	**HFA152a** [13]	**HFO1234ze(E)** [14]
Density (liquid) at 20°C (g/ml)	1.23	1.41	0.91	1.17
Saturated Vapor Pressure at 20°C (bar)	5.72	3.90	5.12	4.27
Boiling Point (°C)	-26.1	-16.5	-24.0	-19.0
Jakob number (at 20°C) [15]	0.43	0.52	0.25	0.37

NON-CONFIDENTIAL

Materials & Methods

Placebo pMDIs containing propellant-only formulations of each propellant in Table 1 were manufactured using 16 mL canisters (Kindeva Drug Delivery, Clitheroe, UK) with 50 µL Bespak valves (Bespak, Kings Lynn, UK). Aerosol sprays were emitted via a Kindeva actuator (Kindeva Drug Delivery, Loughborough, UK) with spray orifice diameter of 0.3 mm and 0.65 mm length.

PIV measurements were undertaken using an Oxford Lasers EnVision Pharma R&D system (Oxford Lasers, Oxford, UK) containing a 300 W, 808 nm fast axis collimated Firefly laser (Oxford Lasers, Oxford, UK) of 5 µs pulse duration illuminating the median plane of the pMDI spray. Image pairs were captured using a Photron FASTCAM Mini WX100 12-bit camera coupled with a AF-S NIKKOR 35mm 1:1.8G lens at aperture f/8, operating at 1 kHz (per image pair) and 2048 x 1024 pixels imaging a 148 x 74 mm region ex-mouthpiece for 150 ms duration. PIV analysis was undertaken using PIVView 2C software version 3.9 (PIVTEC GmbH, Göttingen, Germany).

The EnVision actuator controller was used to actuate the pMDI into free air. Three aerosol units per formulation were primed (three shots), prior to testing in triplicate in a randomised test order. During subsequent data analysis it was found that two spray events of the HFA227ea plume had failed to capture and therefore data presented are an average of seven determinations.

Results & Discussion

Figure 1 and Figure 2 present velocity vector plots of HFA134a and HFA152a sprays at a snapshot in time 25% and 50% through the duration of each spray (on a theoretical mass basis). The highly dynamic nature of the ex-actuator pMDI spray, travelling from left to right, can be seen. Near the mouthpiece exit a narrow, high velocity plume is seen (red-yellow colours). As the plume mixes with entrained air the plume widens and the velocity decays (green-blue colours). Pulses of high velocity droplets within the plume can be seen in each plot corresponding with widening and narrowing of the plume and its changing shape. The richness of the PIV data reveals the transient nature of pMDI sprays both temporally and spatially during a single snapshot in time and throughout the spray event, which cannot be matched by simple plume front velocity tracking measurements.

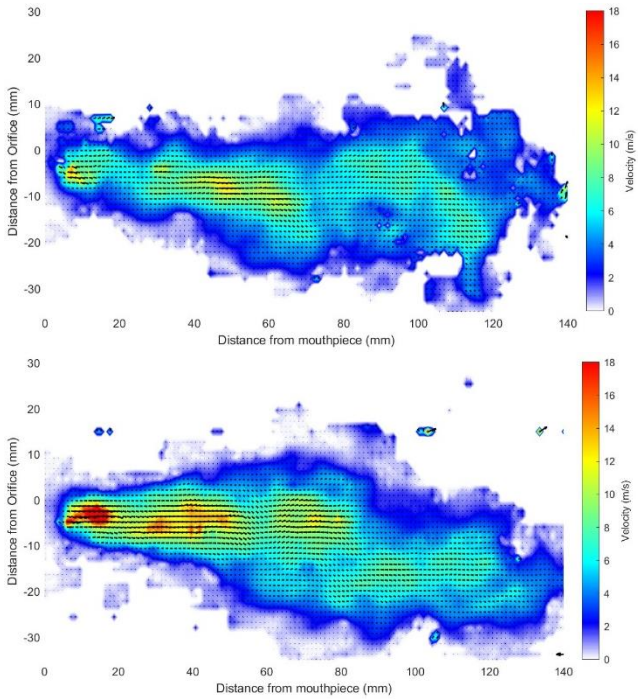


Figure 1: Velocity vector plot of HFA134a spray plume: 25% (top) and 50% (bottom) through spray event

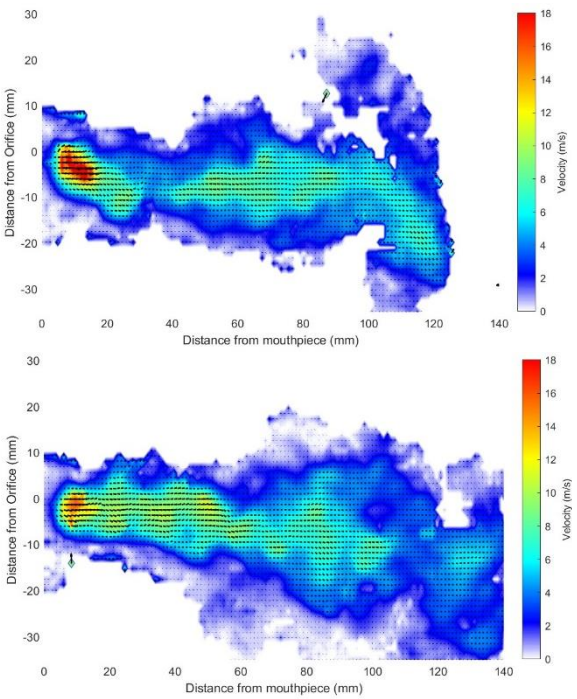


Figure 2: Velocity vector plot of HFA152a spray plume: 25% (top) and 50% (bottom) through spray event

Figure 3 shows an example ensemble average velocity contour plot with the location of the actuator mouthpiece highlighted. Axial velocity through the centreline of the plume is plotted in Figure 4 and the radial profile of axial velocity and temporal axial velocity profile in the centre of the plume 25 mm from the actuator mouthpiece are presented in Figure 5 and Figure 6 as indicated in Figure 3. The location 25 mm downstream of the mouthpiece corresponds roughly to a point within a patient's oral cavity.

NON-CONFIDENTIAL

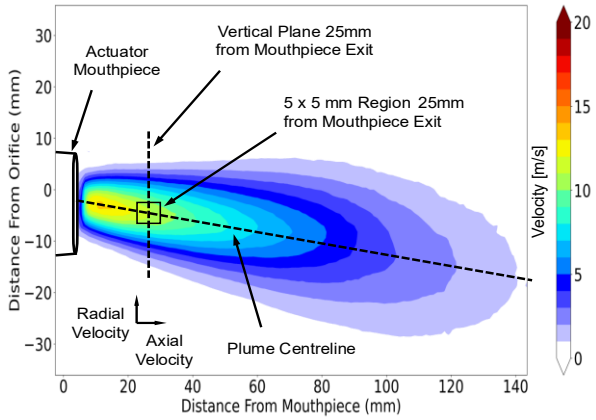


Figure 3: Example ensemble average velocity contour plot

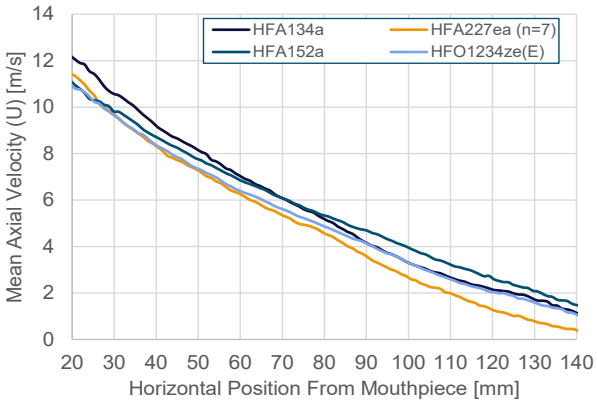


Figure 4: Ensemble averaged axial velocity through plume centreline

Axial Velocity Profile Through Plume Centreline

Figure 4 presents the ensemble averaged axial velocity profile along the centreline of the spray plume. The velocity profiles of each propellant are broadly similar decaying as the plume travels further from the mouthpiece and turbulent mixing with entrained air occurs. The velocity profiles agree well with those previously reported in the literature [6,9]. HFA134a plume velocity was the highest closest to the actuator mouthpiece (20-50 mm) with the velocity of the other propellant sprays all roughly around 10% slower, broadly correlating with HFA134a having the highest vapour pressure driving the initial velocity of the plume. In the region 100-150 mm from the mouthpiece, the rank order of velocity followed HFA152a>HFA134a & HFO1234ze(E)>HFA227ea following the rank order of propellant Jakob number (ratio of sensible to latent heat) which indicates the propensity for droplet evaporation. A lower Jakob number suggests less evaporation is likely and therefore spray momentum will be preserved. The velocity of the HFA152a spray plume decays at the lowest rate of each propellant consistent with its lower Jakob number in Table 1. Overall, the magnitudes of velocities measured were similar.

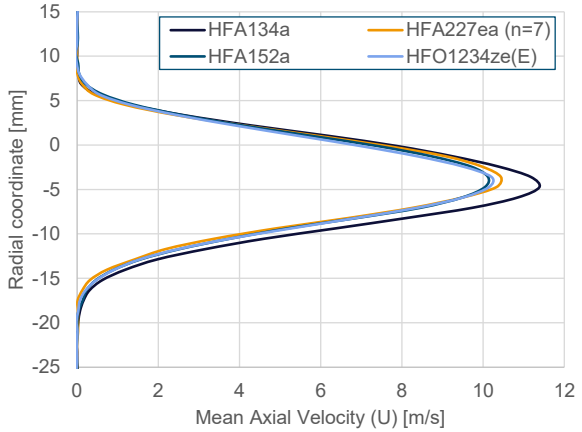


Figure 5: Ensemble averaged axial velocity profile vertically through plume 25 mm from mouthpiece

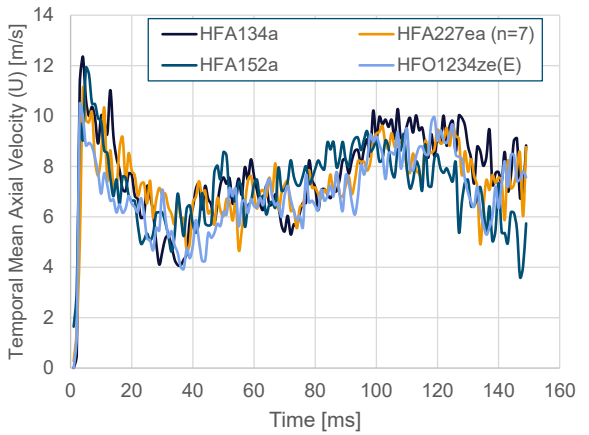


Figure 6: Temporal averaged axial velocity in 5x5 mm centreline region 25 mm from mouthpiece exit plane

Radial Profile of Axial Velocity 25 mm from Mouthpiece Exit

A profile of the axial velocity vertically through the plume 25 mm from the actuator exit plane is presented in Figure 5. The radial profiles of axial velocity of each propellant are broadly similar in shape following a gaussian profile with peak velocities measured in the centre of the spray, in line with previous works in the literature. The width of each of the plumes, based on the velocity distributions were all at this particular measurement distance.

Temporal Velocity Profile 25 mm from Mouthpiece Exit

The temporal velocity profile in a 5x5 mm square region on the plume centreline 25 mm from the mouthpiece exit, corresponding an average of 4x4 vector determinations is presented in Figure 6.The temporal velocity trend and magnitude of each propellant measured are broadly similar.

A sharp rise in velocity as the spray is initiated in the first 5-10 ms was measured as evaporating propellant vapour ejects the initial liquid droplets. This is followed by a rapid reduction of velocity to a minimum around 30-40 ms, as liquid formulation flows from the valve metering chamber into the actuator

NON-CONFIDENTIAL

sump. The fluid quality – mass fraction of vapour to liquid – in the sump reduces, leaving a reduced quantity of vapour to expand and eject the liquid formulation from the spray orifice into the plume. From 40 ms to around 120 ms the velocity of the plume steadily increases, correlating with increasing evaporation of propellant liquid to vapour in the actuator sump, increasing the fluid quality. As the amount of expanding propellant vapour increases, ejecting the liquid formulation droplets, so does the velocity of droplets within the spray plume. At the end of the spray event, as the metered dose is depleted, the remaining propellant formulation has undergone significant evaporative self-cooling reducing its vapour pressure, the driving force by which the final remnants of the liquid formulation are ejected from the pMDI mouthpiece, hence leading to a reduction of plume velocity.

The temporal velocity profiles of each propellant are similar in magnitude, as was expected based on the velocity data in Figure 4 and Figure 5, with no significant differences between any of the propellants.

Conclusions

Velocity profiles of spray plumes of placebo propellant-only pMDIs have been measured using the PIV technique. The profiles of axial velocity through the centreline of the plume, through a vertical plane 25 mm downstream of the mouthpiece exit and temporally in the centre of the plume at the same distance have been plotted to enable comparison of the velocity of each propellant. Generally, the velocity profiles were similar in trend and magnitude with some minor differences observed between each propellant measured. Unlike plume front velocity measurement data, the detailed PIV data captured in this study corroborated literature data documenting the temporal behaviour and spatial distribution and evolution of velocity of HFA134a and HFA227ea propellant sprays. Moreover, the PIV data also revealed the temporal and spatial behaviour of low GWP HFA152a and HFO1234ze(E) propellant sprays were very similar to HFA134a and HFA227ea sprays.

The relative similarity of the velocity profiles of low GWP propellants HFA152a and HFO1234ze(E) compared to those of HFA134a and HFA227ea suggests that broadly similar spray plume behaviours may be expected when switching propellants during redevelopment of pMDI products. Further work would be required to explore the effect on pMDI velocity profiles of inclusion of ethanol co-solvent in the formulation and to determine the effect of pMDI hardware specification such as actuator orifice size

References

[1] J.N. Pritchard, F-Gas Regulations and Beyond: Clinical and Economic Factors that will Drive Propellant Transition, in: Respiratory Drug Delivery, 2020.

[2] P.B. Myrdal, P. Sheth, & S.W. Stein, Advances in metered dose inhaler technology: formulation development. AAPS PharmSciTech, 15(2), 434–455, 2014.

[3] B.J. Myatt, H.K. Versteeg, G.K. Hargrave, E.J. Long, B Gavtash, D.A. Lewis, T Church & G Brambilla, Unlocking further understanding of the atomization mechanism of a pressurized metered dose inhaler. Aerosol Science and Technology, 56(11), 1022–1032. 2022

[4] W.H. Finlay, The Mechanics of inhaled pharmaceutical aerosols: an introduction. Academic Press; 2001.

[5] S.P. Newman, Principles of metered-dose inhaler design. Respiratory Care, 50(9), 1177–1190. 2005

[6] C.A. Dunbar, An experimental and theoretical investigation of the spray issued from a pressurised metered-dose inhaler, PhD Thesis, UMIST, Manchester, UK. 1996.

[7] G. Wigley, H.K. Versteeg & D Hodson, Near-orifice PDA measurements and atomisation mechanism of a pharmaceutical pressurised metered dose inhaler. Proceedings of the 18th Annual Conference on Liquid Atomisation and Spray Systems ILASS-Europe 2002, 165–170. 2002.

[8] B.M. Crosland, M.R. Johnson & E.A. Matida, Characterization of the spray velocities from a pressurized metered-dose inhaler. Journal of Aerosol Medicine and Pulmonary Drug Delivery, 22(2), 85–97. 2009

[9] B.J. Myatt, A Fundamental Study of the Primary Atomisation Mechanism and Aerosol Plume Development of the Pressurised Metered Dose Inhaler, PhD Thesis, Loughborough University. 2017

[10] I. Rossi, W.J. Ganley, P.C.L. Kwok, I. Zadrazil, G. Hassall, O. Michelet, S. Sarrailh, G. Brouet, R. Price & J. Shur. Fundamental properties of propellant aerosols can guide transition to low global warming potential pMDIs: size, velocity and surface charge. Drug Delivery to the Lungs. 2021

[11] Zephex® 134a Brochure. Available at: https://www.kouraglobal.com/applications/medical-propellants/zephex-134a/ Accessed June 2025.

[12] Daikin, SOLKANE 227 pharma Product Information. Available at: https://www.daikinchem.de/product/pharma-propellants/ Accessed June 2025.

[13] Zephex® 152a Overview. Available at: https://www.kouraglobal.com/applications/medical-propellants/zephex-152a/ Accessed June 2025.

[14] Honeywell, Solstice ® ze Refrigerant (HFO-1234ze (E)). Available at: https://www.honeywell-refrigerants.com/europe/wp-content/uploads/2018/11/Honeywell-Solstice%AE-ze-Brochure_EN.pdf . Accessed June 2025.

[15] Lemmon EW, Bell IH, Huber ML, McLinden MO: NIST Standard Reference Database 23: Reference Fluid Thermodynamic and Transport Properties-REFPROP, Version 10.0. National Institute of Standards and Technology, Standard Reference Data Program, Gaithersburg, 2018.

NON-CONFIDENTIAL